

Imaging Suzuki Precipitates on NaCl : Mg²⁺ (001) by Scanning Force Microscopy

Clemens Barth* and Claude R. Henry

CRMCN-CNRS, Campus de Luminy, case 913, 13288 Marseille Cedex 09, France[†]

(Received 4 October 2007; published 3 March 2008)

We present a dynamic scanning force and Kelvin microscopy study of Suzuki precipitates on clean (001) surfaces of UHV cleaved NaCl : Mg²⁺. Nanometer sized precipitates with a rectangular shape on flat terraces and also at steps were found. Images with atomic resolution confirm that the precipitates are embedded in the NaCl matrix and permit the identification of each type of ion in the unit cell of the Suzuki structure. Kelvin microscopy images show always a strong bright contrast at the precipitates, which is probably due to the negative cation vacancies in the Suzuki structure.

DOI: [10.1103/PhysRevLett.100.096101](https://doi.org/10.1103/PhysRevLett.100.096101)

PACS numbers: 68.35.B-, 68.35.Dv, 68.37.Ps, 68.55.Ln

Because of their insulating character, the (001) surfaces of alkali halide bulk crystals have been frequently used as substrates for molecules and metal nanoclusters in nanotechnology [1–4]. In order to engineer such surface systems, the influence of the surface on the supported nano-objects must be well known at the atomic scale, which requires a good knowledge and precise handling of the properties of the clean surface. It is well known that impurities in an ionic material can strongly modify the structure, composition, and charge state of its surfaces [5]. For pure crystals for instance, already a small amount of impurity ions in the ppm range strongly determines the charge state of the crystal surfaces due to the surface double-layer mechanism [6]: because most crystals contain divalent impurity cations, a net negative surface charge formed by monovalent cation vacancies at kinks is present [7,8], which influences the electronic properties of supported gold nanoclusters [9].

By a controlled choice of the impurity content, the surface can be tailored in its atomic structure in that it offers new and interesting properties. For instance, if a certain threshold of impurity content is exceeded, the precipitation of additional new phases appears resulting in a nanostructuring of the surface. One famous phase for NaCl like crystals is the Suzuki phase, which was already observed in the 1950s [10] and mainly discussed by Kazuo Suzuki for NaCl : Cd²⁺ crystals [11]. The main characteristic of this phase is its cubic structure being twice as large as the one of NaCl [11–13], the high concentration of ordered cation vacancies and the inclusion of Suzuki precipitates in the NaCl matrix [14,15]. The composition is given by Na₆CdCl₈, where the NaCl lattice serves as a host for Cd²⁺ ions and Na⁺ vacancies occupying alternately Na⁺ corners of the original NaCl unit cell. The anion sublattice (Cl⁻) is identical to the one in the NaCl unit cell, whereas the Na⁺ ions are unchanged at the centers of the faces. Many Suzuki phases have been studied with various different types of divalent impurity ions (Cd²⁺ [11,13,15,16], Mn²⁺ [14,17], Mg²⁺ [12,16,18], Fe²⁺ [12]). The host lattice must not necessarily be NaCl; the

Suzuki phase was also observed in LiCl(: Mg²⁺, V²⁺, Mn²⁺) [19], in LiF:Mg²⁺ [20], and even in oxides (MgO : Mn⁴⁺ and NiO : Mn⁴⁺ [10,21]).

Although nanostructured surfaces with Suzuki precipitates might be promising substrates for nano-objects and although a large amount of work has been devoted to the Suzuki phase, a microscopy study at atomic scale of these surfaces is still missing. The latter can be principally done by dynamic scanning force microscopy (dynamic SFM), which permits imaging of surfaces with true atomic resolution [22–24]. The microscope can be combined with the Kelvin modulation technique, which visualizes the electrostatic surface potential at nanometer scale [8,25,26]. In this Letter, dynamic SFM and Kelvin probe force microscopy (KPFM) measurements of clean NaCl : Mg²⁺ (001) crystal surfaces with nanometer sized Suzuki precipitates are presented. Both the atomic structure and the surface charge state of the Suzuki precipitates are involved.

NaCl crystals were grown in an argon atmosphere by the Czochralski growth method and were doped with Mg²⁺ ions (99% NaCl, 1% MgCl₂) [15]. The surfaces were prepared by UHV cleavage at room temperature followed by annealing in an UHV oven up to 220 °C [26,27]. A speed not higher than 6 °C/min was used for the annealing and cooling. Experiments were performed in the low 10⁻¹⁰ mbar pressure range and at room temperature with a dynamic SFM (Omicron STM/AFM, nanoSurf digital demodulator). A conductive silicon cantilever from Nanosensors (*p*-Si, 0.015 Ω cm, 318 kHz, 37 N/m) was used. Because the silicon tip was originally exposed to the atmosphere, it was covered by an oxide layer. For the Kelvin microscope, a dc (U_{dc}) and ac voltage (U_{ac}) are applied in series at the rear side of the sample (tip at ground) [26]. During scanning, the electrostatic tip-surface interaction between tip and surface is minimized at each point on the surface by applying a voltage $U_{dc,0}$. Images of the latter voltage represent the electrostatic surface potential [8,25,26].

In Figs. 1(a) and 1(b) a topography and corresponding Kelvin image are shown, respectively, which were re-

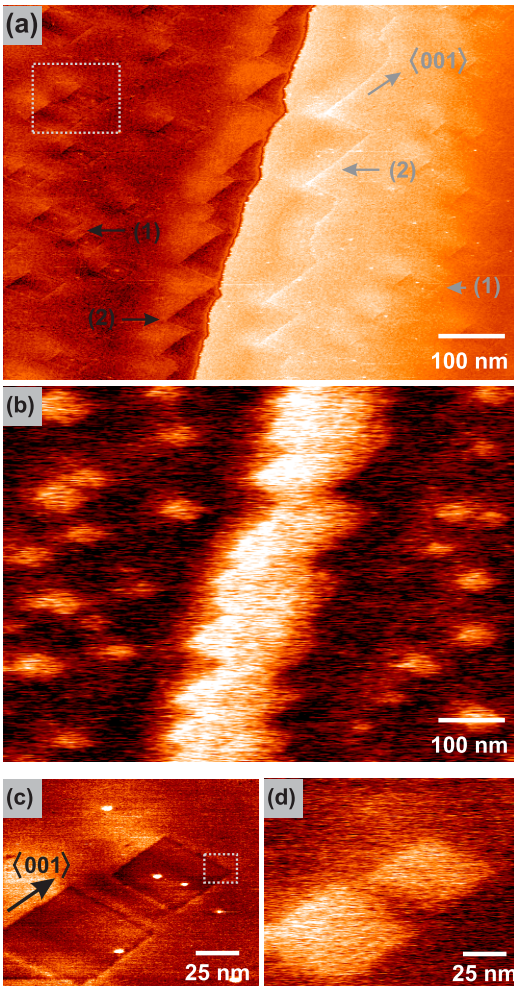


FIG. 1 (color online). Topography (a) and corresponding Kelvin image (b) of a (001) surface of a NaCl : Mg²⁺ crystal, which was cleaved and annealed in UHV. Topography (c) and Kelvin image (d) of the surface region labeled by the dotted rectangular in image (a). $A_{p-p} = 23$ nm, $\Delta f = -32$ Hz, $U_{ac} = 0.8$ V, $f_{ac} = 474$ Hz; (a),(b) 770×560 nm²; (c),(d) 140×115 nm².

corded simultaneously during one KPFM measurement. The images show the (001) surface of a NaCl : Mg²⁺ crystal after its preparation. Apart from the double-layer step in the middle of the topography image [1(a)], small well-separated patches on the large terraces (e.g., at 1) can be observed. In order to inspect these patches more in detail, a Kelvin measurement in the small surface region, which is marked by the white dotted rectangle in Fig. 1(a), was performed. The topography and corresponding Kelvin image are shown in Figs. 1(c) and 1(d), respectively. The patches seem to be depressions of ~ 80 pm [1(c)], which is below the smallest possible unit block of NaCl (2.8 Å). Although the shape of the patches was rectangular, the patches exhibit, however, a trapezoidal shape in the images, which was a result of the long image acquisition time of 35 min ($\nu_{Scan} = 0.5$ Hz) and the instrumental drift of the piezoscanner. The patches appear with a density of

4.9×10^9 patches/cm² in this surface region and have <001> edges with lengths between 25 and 60 nm. In the vicinity of the double-layer step [1(a)], the same type of patches can be found forming a fringe with a zig-zag shape around the step [e.g., at 2 in Fig. 1(a)]. The corresponding Kelvin image [1(b)] exhibits a strong bright contrast at all rectangular patches and at the zigzag shaped fringe of the step. The bright Kelvin contrast belongs to more positive bias voltages (voltage difference ~ 1.0 V) with respect to dark regions on the flat terraces and is uniform over the whole area of each patch as it can be seen in image (d) in Fig. 1.

The same type of patches with a bright Kelvin contrast were found at many other positions on the crystal surface, even after several days. Sometimes large surface regions with a corresponding bright Kelvin contrast as shown in Fig. 2 were found. These regions belonged either to complete terraces (1) or were visible on one single terrace, where the Kelvin contrast changed from black to white at some position on the terrace (compare 2 with 3). In most cases, patches could be found especially at steps.

All observations described so far coincide well with the ones that were made by transmission electron microscopy (TEM) on the same type of surface [18] and on (001) surfaces of NaCl : Mn²⁺ [14] and NaCl : Cd²⁺ [15]: The rectangular patches and the patches at steps are indeed Suzuki precipitates. The rectangular precipitates with <001> boundaries in Fig. 1 could obviously appear due to the small step density in this surface region [15]. In contrast, the precipitates at the steps in Fig. 2 were probably prohibited from forming straight <001> boundaries due to the high step density in this surface region [15]. As will be shown below, the surface potential changes above the precipitates, which produces a bright Kelvin contrast.

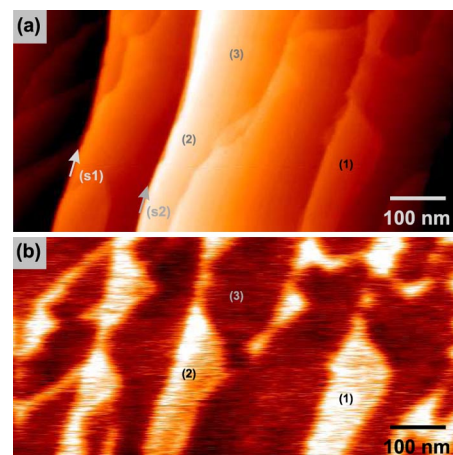


FIG. 2 (color online). The same crystal surface as shown in Fig. 1 at another position. The topography and corresponding Kelvin signal are shown in (a) and (b), respectively. The steps (s1) and (s2) have a height of ~ 2 nm, all other steps are single or double monoatomic high steps. 800×402 nm², $A_{p-p} = 23$ nm, $\Delta f = -35$ Hz, $U_{ac} = 1.5$ V, $f_{ac} = 474$ Hz.

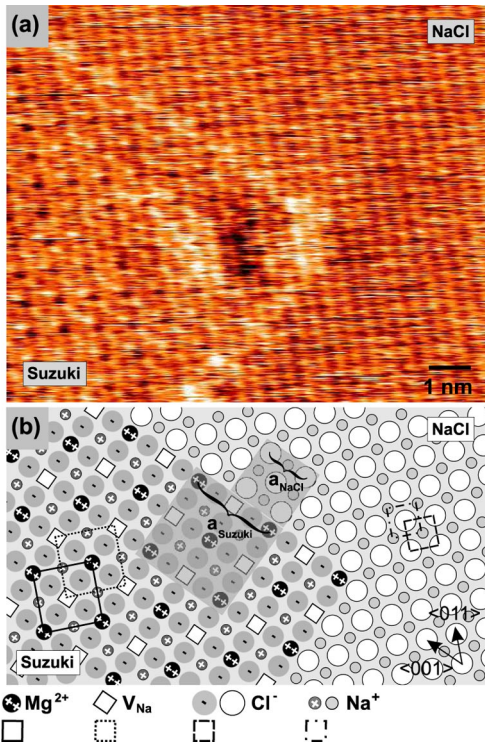


FIG. 3 (color online). (a) Detuning image with atomic resolution of the corner of a Suzuki precipitate that was taken in the surface region marked by the white dotted square in image (c) of Fig. 1. The rectangular shape of the precipitate appears much less distorted than in the images of Fig. 1, which was due to the considerably higher scanning speed of 12 Hz ($12 \times 10 \text{ nm}^2$, $A_{p-p} = 23 \text{ nm}$, $\Delta f = -177 \text{ Hz}$). (b) Drawing of the expected Suzuki phase inside the NaCl matrix.

In order to study the Suzuki precipitates at atomic scale they were imaged with a higher resolution in the constant height mode without the Kelvin modulation. An image with atomic resolution is shown in Fig. 3(a), which was recorded in the surface region marked by the dotted rectangular in Fig. 1(c). The corner of the precipitate is on the left side; the right surface region belongs to pure NaCl(001). Because both regions exhibit same mean detuning values (same mean color), it can be concluded that the two regions are almost on the same height level in the z direction—the depressions in the topography images (a) and (c) of Fig. 1 were a result of a residual electrostatic tip-surface interaction that was not completely minimized in the KPFM measurements. The ionic lattice inside the precipitate, which is represented by dark spots, is twice as large as the one on NaCl(001), which is mainly formed by bright ions. A distance of $(4.1 \pm 0.3) \text{ \AA}$ between bright ions on NaCl(001) was found, which is in agreement with the next-neighbor distance of $a_{\text{NaCl}}/\sqrt{2} = 3.96 \text{ \AA}$ for ions of the Cl^- or Na^+ sublattice in NaCl. Therefore, the bright ions are addressed as either Na^+ or Cl^- ions [28]. The right side of the drawing in Fig. 3(b) shows the NaCl(001) region and the corresponding Cl^- and Na^+ ions with their two sublattices (small dashed and dot-dashed squares). On

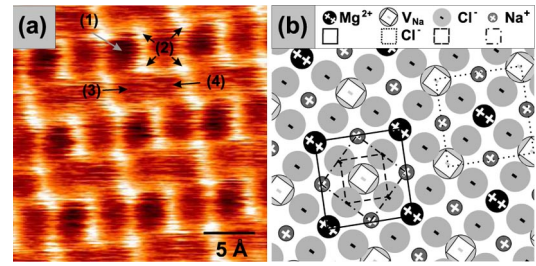


FIG. 4 (color online). (a) Detuning image with atomic resolution of a Suzuki precipitate (recorded without Kelvin modulation). $3.3 \times 3.3 \text{ nm}^2$, $A_{p-p} = 46 \text{ nm}$, $\Delta f = -24.9 \text{ Hz}$. (b) Drawing explaining the atomic structure of the precipitate.

the left, a corner formed by the $\langle 001 \rangle$ edges of the precipitate in its expected Suzuki structure is drawn. The projection of the unit cell is given by the large gray square, which has a lattice constant of $a_{\text{Suzuki}} = 2a_{\text{NaCl}} = 11.39 \text{ \AA}$ being twice as large as the one of NaCl (small gray square) [12,13]. A comparison with the experimental image inside the precipitate can be addressed either to the Mg^{2+} sublattice (full line square) or to the one of the vacancies (dotted square).

The detuning image in Fig. 4(a) shows the atomic details of the precipitate with a higher resolution. Although an unambiguous identification of the atomic contrast needs a comparison with theory [23], it can be estimated with good certainty how the atomic contrast is formed—thanks to the geometry of the Suzuki phase [29]. The dark spots (e.g., at 1) but also additional bright spots (e.g., at 2) forming a sublattice, which is parallel to the one of the dark spots but half as large, can be clearly seen. Because the smallest possible sublattice of the Suzuki phase is formed by the Cl^- ions [see Fig. 4(b)] and because this lattice coincides with the one of the bright ions, the bright ions (2) can be addressed to the chlorine ions. This has the important consequence, that the tip's last atom had obviously a negative potential producing a repulsive interaction with the Cl^- ions [28]. In contrast to the Cl^- ions, the divalent positive Mg^{2+} and monovalent positive Na^+ ions should be imaged in a darker contrast [28]. Therefore, it is anticipated that the darkest spots (1) belong to the Mg^{2+} ions because they should exhibit a stronger interaction with the tip than the Na^+ ions. The latter Na^+ ions have to be always in between two dark Mg^{2+} ions and are surrounded by four bright Cl^- ions. The contrast should be less dark than at the Mg^{2+} ions but also less bright than at the Cl^- ions [28]. Indeed, between two dark Mg^{2+} ions gray sites (3) can be found in the experimental image forming the expected quadratic sublattice as shown in image [4(b)], which is smaller than the Mg^{2+} lattice but larger than the Cl^- one and rotated by 45° with respect to the Cl^- and Mg^{2+} lattices. The vacancies must be located in the middle of a Mg^{2+} square, where also a gray contrast can be found (4) in the experimental image. It can be speculated that this

contrast is due to the Cl^- ions in the second layer below the vacancies, which distance to the tip is 2.8 Å larger with respect to ions of the first layer. Because atomic resolution imaging is based on the short-range chemical tip-surface interaction with typical tip-surface distances of a few Ångströms [23], the interaction of the second layer Cl^- ions with the tip is considerably less strong than in the case of the Cl^- ions of the first layer.

The vacancies play probably an important role in the Kelvin contrast formation. If the net positive and negative valences of the ions in the first layer are counted, the same number of net positive and negative valences is obtained [e.g. in one Mg^{2+} square in Fig. 4(b): $4 \times \text{Cl}^- \Leftrightarrow 2 \times \text{Na}^+ + 1 \times \text{Mg}^{2+}$]. However, below the vacancies, the negative Cl^- ions in the second layer are present. Because the Kelvin microscope is sensitive to long-range electrostatic forces (tip-surface distance: 1–3 nm), it can be assumed that the additional “unscreened” Cl^- ions in the second layer modify the surface potential in that a bright Kelvin contrast is imaged. A bright Kelvin contrast belongs indeed to something more negative, which means that the surface carries a net negative charge being roughly similar to the case described before [8]. The high density of vacancies (or second layer Cl^- ions) would then explain the uniform and high Kelvin contrast of 1 V—the tip integrates the electrostatic interaction over many vacancy sites of a large surface area, which is comparable to the tip dimension.

In conclusion, Suzuki precipitates on $\text{NaCl} : \text{Mg}^{2+}(001)$ surfaces were studied by dynamic SFM for the first time. Atomically resolved images show the expected atomic structure but also the inclusion of the precipitates in the NaCl matrix. Thanks to the special geometry of the Suzuki phase, each type of ion within the unit cell could be identified. Kelvin measurements show always a bright Kelvin contrast above the precipitates which probably originates from the cation vacancies. We believe that Suzuki precipitates are suitable to calibrate the potential of the tip’s last atom, which is important for the atomic contrast interpretation in general [23]. However, more importantly we believe that the nanostructured surfaces are very promising templates for nano-objects like nano-clusters [15] on which we will concentrate in the future.

We thank G. Grange for the crystals. Fruitful discussion with A. S. Foster are highly acknowledged. This work was supported by the European Community through the STRP GSOMEN and by the European COST program through Action D41.

*To whom all correspondence should be addressed.
barth@crmcn.univ-mrs.fr

†The CRMCN is associated with the Universities of Aix-Marseille II and III.

- [1] L. Nony *et al.*, Nano Lett. **4**, 2185 (2004).
- [2] J.M. Mativetsky, S.A. Burke, S. Fostner, and P. Grütter, Small **3**, 818 (2007).
- [3] Z. Gai, J.Y. Howe, J. Guo, D.A. Blom, E.W. Plummer, and J. Shen, Appl. Phys. Lett. **86**, 023107 (2005).
- [4] M. Goryl, F. Buatier de Mongeot, F. Krok, A. Vevecka-Priftaj, and M. Szymonski, Phys. Rev. B **76**, 075423 (2007).
- [5] W. Hayes and A.M. Stoneham, *Defects and Defect Processes in Nonmetallic Solids* (Dover Publications, Inc., Mineola, NY, 1985).
- [6] J. Frenkel, *Kinetic Theory of Liquids* (Clarendon Press, Oxford, 1946).
- [7] K.L. Kliewer and J.S. Koehler, Phys. Rev. **140**, A1226 (1965).
- [8] C. Barth and C.R. Henry, Phys. Rev. Lett. **98**, 136804 (2007).
- [9] C. Barth and C.R. Henry, Appl. Phys. Lett. **89**, 252119 (2006).
- [10] J.S. Kasper and J.S. Prenner, Acta Crystallogr. **7**, 246 (1954).
- [11] K. Suzuki, J. Phys. Soc. Jpn. **10**, 794 (1955); **16**, 67 (1961).
- [12] C.J.J. van Loon and D.J.W. Ijdo, Acta Crystallogr. Sect. B **31**, 770 (1975).
- [13] M. Chall, B. Winkler, P. Blaha, and K. Schwarz, J. Phys. Chem. B **104**, 1191 (2000).
- [14] G.A. Bassett and M.J. Yacaman, Thin Solid Films **31**, 375 (1976).
- [15] G. Grange, Surf. Sci. **105**, 265 (1981).
- [16] N. Bonanos and E. Lilley, Mater. Res. Bull. **14**, 1609 (1979).
- [17] M. Moreno, J.C. Gómez Sal, J. Aramburu, F. Rodríguez, J.L. Tholence, and F. Jaque, Phys. Rev. B **29**, 4192 (1984).
- [18] A.L. Guerrero, E.P. Butler, P.L. Pratt, and L.W. Hobbs, Philos. Mag. A **43**, 1359 (1981).
- [19] C. Cros, L. Hanebali, L. Latié, G. Villeneuve, and W. Gang, Solid State Ionics **9–10**, 139 (1983).
- [20] E. Lilley and J.B. Newkirk, J. Mater. Sci. **2**, 567 (1967).
- [21] P. Porta, G. Minelli, I.L. Botto, and E.J. Baran, J. Solid State Chem. **92**, 202 (1991).
- [22] S. Morita, R. Wiesendanger, and E. Meyer, *Noncontact Atomic Force Microscopy* (Springer-Verlag, Berlin, 2002).
- [23] W.A. Hofer, A.S. Foster, and A.L. Shluger, Rev. Mod. Phys. **75**, 1287 (2003).
- [24] R. Hoffmann, L.N. Kantorovich, A. Baratoff, H.J. Hug, and H.-J. Güntherodt, Phys. Rev. Lett. **92**, 146103 (2004).
- [25] Y. Rosenwaks, R. Shikler, Th. Glatzel, and S. Sadewasser, Phys. Rev. B **70**, 085320 (2004).
- [26] C. Barth and C.R. Henry, Nanotechnology **17**, S155 (2006).
- [27] C. Barth, C. Claeys, and C.R. Henry, Rev. Sci. Instrum. **76**, 083907 (2005).
- [28] The atomic contrast depends on the potential of the tip’s last atom [23]. If the potential is negative, the interaction is attractive above the cations (dark contrast) and repulsive above the anions (bright contrast), and vice versa.
- [29] Recent numerical simulations strongly support our contrast interpretation. A.S. Foster (private communication).